AD-A248 350

92-09484

(2)

REPORT DOCUMENTATION PAGE

Form Approved OMB No. 0704-0188

1a. REPORT SECURITY CLASSIFICATION: UNCLASSIFIED	1b. RESTRICTIVE MARKINGS: NONE
2a. SECURITY CLASSIFICATION AUTHORITY	3. DISTRIBUTION/AVAILABILITY OF REPORT: APPROVED FOR PUBLIC RELEASE AND SALE: ITS DISTRIBUTION IS UNLIMITED.
2b. DECLASSIFICATION/DOWNGRADING SCHEDULE	
4. PERFORMING ORGANIZATION REPORT NUMBER(S): Technical Report No. 003	5. MONITORING ORGANIZATION REPORT NUMBER(S)
6a. NAME OF PERFORMING ORGANIZATION: UNIVERSITY OF TEXAS AT AUSTIN; 6b. OFFICE SYMBOL (If applicable)	7a. NAME OF MONITORING ORGANIZATION: DEPARTMENT OF SPONSORED PROJECTS, THE UNIVERSITY OF TEXAS AT AUSTIN
6c. ADDRESS (City, State, and ZIP Code): Department of Chemical Engineering, Austin, Texas 78712-1062	7b. ADDRESS (City, State, and ZIP Code): P. O. BOX 7726, AUSTIN, TX 78713-7726
8a. NAME OF FUNDING/SPONSORING ORGANIZATION: OFFICE OF NAVAL RESEARCH; 8b. OFFICE SYMBOL (If applicable)	9. PROCUREMENT INSTRUMENT IDENTIFICATION NUMBER
8c. ADDRESS (City, State, and ZIP Code): 800 N. QUINCY STREET, ARLINGTON, VA 22217	10. SOURCE OF FUNDING NUMBERS: PROGRAM ELEMENT NO. / PROJECT NO. / TASK NO. / WORK UNIT ACCESSION NO.

11. TITLE (Include Security Classification): L-α-Glycerophosphate and L-Lactate Electrodes Based on the Electrochemical "Wiring" of Oxidases. UNCLASSIFIED

12. PERSONAL AUTHOR(S): Ioanis Katakis and Adam Heller

13a. TYPE OF REPORT	13b. TIME COVERED	14. DATE OF REPORT (Year, Month, Day)	15. PAGE COUNT
Technical	FROM 10/91 TO 3/92	1992 March 20	2

16. SUPPLEMENTARY NOTATION

17. COSATI CODES			18. SUBJECT TERMS (Continue on reverse if necessary and identify by block number)
FIELD	GROUP	SUB-GROUP	Electrodes; Electrochemistry; Oxidases; Enzymes.

19. ABSTRACT (Continue on reverse if necessary and identify by block number)

The title electrodes were constructed by co-immobilizing the respective FAD oxidases on solid electrode surfaces with a poly(vinyl pyridine) polymer which was N-derivatized with bromo ethylamines and $Os(bpy)_2Cl_2$. The redox-polymer - enzyme hydrogels were crosslinked on the electrode surface using poly(ethylene glycol) diglycidyl ether. As in the case of glucose oxidase, the redox polymer acts as an electron relaying "wire" transferring electrons directly from the enzymes' $FADH_2$ centers to the electrode. This transfer competes with the natural process of reoxidation of the $FADH_2$ by molecular oxygen. The (cont.)

20. DISTRIBUTION/AVAILABILITY OF ABSTRACT: ☐ UNCLASSIFIED/UNLIMITED ☐ SAME AS RPT ☐ DTIC USERS	21. ABSTRACT SECURITY CLASSIFICATION: UNCLASSIFIED
22a. NAME OF RESPONSIBLE INDIVIDUAL: Adam Heller	22b. TELEPHONE (Include Area Code): (512) 471-8874; 22c. OFFICE SYMBOL

DD Form 1473, JUN 86 — Previous editions are obsolete. — SECURITY CLASSIFICATION OF THIS PAGE: UNCLASSIFIED

Box 19 (continued)

variation of the response of these electrodes with the atmosphere (N_2 or air), pH, and substrate concentration was determined. The pH profile of the electrocatalytic current differs from that of the activity of the free enzymes, exhibiting a broader maximum, shifted to higher pH values. The observed sensitivities and linear ranges are respectively : $2X10^{-2}$ A M^{-1} cm^{-2} and 2.7 mM for L-a-glycerophosphate, and 0.3 A M^{-1} cm^{-2} and 0.2 mM for l-lactate that may be compared to $2X10^{-2}$ A M^{-1} cm^{-2} and 10 mM for glucose. The 0-90% response time for all electrodes is 1 sec or less.

L-α-GLYCEROPHOSPHATE AND L-LACTATE ELECTRODES BASED ON THE ELECTROCHEMICAL "WIRING" OF OXIDASES

Ioanis Katakis and Adam Heller*
The University of Texas at Austin, Department of Chemical Engineering
Austin, Texas 78712

ABSTRACT

The title electrodes were constructed by co-immobilizing the respective FAD oxidases on solid electrode surfaces with a poly(vinyl pyridine) polymer which was N-derivatized with bromo ethylamines and $Os(bpy)_2Cl_2$. The redox-polymer - enzyme hydrogels were crosslinked on the electrode surface using poly(ethylene glycol) diglycidyl ether. As in the case of glucose oxidase, the redox polymer act as an electron relaying "wire" transferring electrons directly from the enzymes' $FADH_2$ centers to the electrode.This transfer competes with the natural process of reoxidation of the $FADH_2$ by molecular oxygen . The variation of the response of these electrodes with the atmosphere (N_2 or air), pH, and substrate concentration was determined. The pH profile of the electrocatalytic current differs from that of the activity of the free enzymes, exhibiting a broader maximum, shifted to higher pH values. The observed sensitivities and linear ranges are respectively : $2X10^{-2}$ A M^{-1} cm^{-2} and 2.7 mM for L-α-glycerophosphate, and 0.3 A M^{-1} cm^{-2} and 0.2 mM for l-lactate that may be compared to $2X10^{-2}$ A M^{-1} cm^{-2} and 10 mM for glucose. The 0-90% response time for all electrodes is 1 sec or less.

INTRODUCTION

In contrast with low molecular weight polymers that diffusionally mediate electron transfer from the enzymes' active center *(1-3)* to electrodes, high molecular weight polymers can be designed to complex with redox enzyme proteins, and to non-diffusionally relay electrons from the enzyme redox centers to electrodes. In these complexes, the oxidized redox polymers compete efficiently with oxygen in the oxidation of substrate reduced enzyme redox centers *(4-6)*. The high molecular weight redox polymers connect the enzyme redox centers to electrodes only when they (a) are adsorbed on the electrodes and (b) have long non-absorbed segments extended into the solution that complex and penetrate enzyme proteins. These superficially contradictory requirements are

met by making the molecular weight high enough so that even though most segments are most of the time unadsorbed, i.e. in solution, there is always a sufficient number of segments adsorbed to make their simultaneous desorption statistically improbable. In the special case of crosslinkable enzyme-complexing polymers, three-dimensional, enzyme-incorporating hydrophilic networks of molecular weights greatly exceeding those of either the constituent redox polymer or of the enzyme can be formed on electrode surfaces (*7-11*).

We show here that in addition to redox centers of glucose oxidase (*11*) also redox centers of glycerophosphate oxidase, and lactate oxidase can be electrochemically connected to electrodes through crosslinked redox polymer-enzyme hydrophilic epoxy networks and characterize the resulting glycerol - 3 - phosphate and lactate electrodes.

EXPERIMENTAL SECTION

Chemicals. L-α-glycerol phosphate oxidase (GPO) (l-α-glycerophosphate : oxygen oxidoreductase, EC 1.1.3.21) from Aerococcus viridans, and lactate oxidase (LOX) (l-lactate : oxygen oxidoreductase, former EC 1.1.3.2) from Pediococcus species, were purchased from Genencor Int (representatives of Toyo Jozo) and were used without purification. Glucose oxidase (GOX) (D-glucose : oxygen oxidoreductase, EC 1.1.3.4) from Aspergillus niger, and peroxidase (Donor: H_2O_2 oxidoreductase, EC 1.11.1.7) from horseradish were purchased from Sigma (catalog numbers G-7141 and P-8250 respectively) and were also used without purification. L-lactic acid and D,L -α- glycerophosphate were also purchased from Sigma. D-glucose was purchased from J.T. Baker. All other chemicals (phenol, o-dianisidine, 4-aminoantipyrine) were of reagent grade or better and were purchased either from Sigma or Aldrich. Water used was NANOpure® and the buffer most commonly employed was 33 mM phosphate, .15 M NaCl at pH 7.15 (to be referred to as STD buffer). The redox polymer (linear PVP of approximately 50 Kda N-derivatized with $Os(bpy)_2Cl_2$ and bromoethylamine as reported earlier) had an approximate equivalent MW per osmium center of 1510 as determined by elemental analysis and UV spectrophotometry (*11*). The diepoxide used was poly(ethylene glycol) diglycidyl ether purchased from Polysciences (cat # 08210).

Electrodes. Modified electrodes were glassy carbon discs, 3 mm in diameter (V-10 grade vitreous carbon from Atomergic). The glassy carbon rods were encased in teflon cylinders with deaerated slow setting epoxy (Armstrong) and the teflon cylinder was fitted on an AFMSRX rotator (Pine Instruments).

All electrodes were treated by polishing on three grits of sand paper and then successively on four grades of alumina (20, 5, 1, .3 micron) with sonication and thorough washing with NANOpure® water between grades. Background scans for every electrode were taken at 1000, 500 and 100 mV/s in STD buffer to make sure the voltammograms were featureless. The

electrodes were subsequently washed and stored in a desiccator until use. The average capacitance of the GC electrodes in STD buffer was 29 +/- 5 $\mu F/cm^2$.

The modification procedure was similar to that reported earlier (*11*). Electrodes were prepared either by depositing the components sequentially and mixing on the electrode surface, or (in the case of diffusion studies) from a common mix of enzyme, polymer and crosslinker when reproducibility was important. The weight ratios of enzyme protein to non enzymatic material (contaminants from the enzyme isolation process) to polymer were 1: 3 : 5 for LOX and 1.5 : 0.5 : 5 for GPO electrodes, so as to keep the operation of the electrodes in the kinetically limited regime (see discussion section) and/or to keep the observed current densities at saturating substrate concentrations similar for both types of electrodes. The mixtures contained 6 % (per weight) of crosslinker. For a typical electrode a total of about 8 μg of material yielding a geometric surface coverage of 130 $\mu g/cm^2$ was applied on the surface. The dry thickness of such electrodes was about .8 μm as determined by profilometry and SEM. The electrodes were left to cure in a desiccator for 24 hours under reduced pressure. Before use they were washed by incubation in STD buffer for at least 8 hrs (in 2 ml volume) under vigorous stirring. The solutions in which the electrodes were washed were assayed for enzymatic activity and protein content (see below). There was no effort made to optimize the immobilization procedure, or the current efficiency or the competition with O_2; Rather the goal was to keep the crosslinking conditions as constant and reproducible as possible. Because the GPO or LOX solutions even in 10 mM HEPES buffer at pH 8.1 are not particularly stable, an effort was made to test all the electrodes during the same 12-24 hour period. This requirement was particularly important for the enzymes (other than glucose oxidase) that lost activity during the curing process. The reproducibility of the response of electrodes prepared from the identical enzyme-polymer mixtures was +/- 10% or better, as evidenced by the scatter in both maximum current density at saturating substrate concentration and the concentration at which half the maximum current density was observed ("apparent K_m" or "half saturation point").

Electrochemistry. The electrochemical experiments were performed with a Princeton Applied Research 173 potentiostat, an 175 PAR universal programmer equipped with a model 179 digital coulometer. Signals were recorded on an X-Y-Y' Kipp Zonnen recorder. The chronoamperometric and chronopotentiometric experiments, as well as cyclic voltammetry at less than 1mV/s were performed with the help of a 273 PAR potentiostat interfaced to an IBM PC. Unless otherwise noted, a single compartment water jacketed 100 ml cell was used thermostated at 21.8 +/- .2 °C, with an aqueous saturated calomel electrode as reference (SCE) and all potentials are reported with respect to this. A platinum wire encased in a heat shrinkable sleeve with a frit was used as the counter electrode.

Unless otherwise stated the steady state current was monitored with the electrodes poised at .45 V, where the current no longer varied with potential (The current plateau was reached at about .39 V). Concentrations of L-α-glycerophosphate were calculated from the optical rotation of D,L-α-glycerophosphate. For the GOX electrodes, concentrations of D-glucose are reported even though the enzyme only catalyzes the reaction of the β,D-glucose comprising about 60% of the total D-glucose concentration after mutarotation is complete.

Assays. The activity of the enzymes was determined in all cases at 22 +/- 1°C. A series of experiments with a single enzyme normally took about 3-4 days to complete. During this period, the native enzyme stored dissolved in pH 8.1 10 mM HEPES buffer was periodically assayed for loss of activity under the storage conditions . Concentrations of enzyme solutions were determined from the extinction coefficients of bound FAD in GOX and GPO (*12-15*) (21.6 and 11.3 $mM^{-1}cm^{-1}$ respectively) .For LOX the manufacturer's specification for protein content was accepted. However, after purification of the enzyme through HPLC, it was found that the specific activity and protein content increased fourfold. For determining the total amount of protein , the Biorad microassay method was used (*16*).

The enzyme assays as well as the electrochemical measurements were performed, unless otherwise stated, in STD buffer of pH 7.15. The enzyme assays involved the peroxidase catalyzed reaction of an oxidizable dye, o-dianisidine in the case of GOX , 4-aminoantipyrine and phenol in the case of GPO , and 4-aminoantipyrine and N,N-dimethylaniline in the case of LOX . Absorbances were measured at 500 nm for the former and 565 for the later and the known extinction coefficients were used for quantitation (*17*). The O_2-saturated total reaction volume was generally about 3 ml, and the dyes, substrate, and peroxidase were present in excess. The mean specific activities of the purified enzymes used were 24 units/mg for GPO and 108 units/mg for LOX .

RESULTS AND DISCUSSION

Results. Figure 1 shows that lactate and glycerol-3-phosphate, like glucose, are electrocatalytically oxidized at electrodes coated with 3-dimensional redox polymer epoxy networks incorporating the respective oxidases. The two electrodes were made with different enzyme : non-enzymatic material : polymer weight ratios, 1.5 : 0.5 : 5 for GPO, 1 : 3 : 5 for LOX so as to make their current densities at high substrate concentrations - where these no longer affect the current- similar. The loading was 100 - 130 $\mu g/cm^2$ of the enzyme containing epoxy. The current densities of the resulting electrodes, at high substrate concentrations, were within about 20 %. This condition, achieved experimentally by trial and error, represents a specific set of constituent ratios. Comparison of electrodes made with different enzymes must be based on electrodes with similar

enzyme to polymer ratios (because the protein is an insulator and electron transport is through the redox polymer), and also with similar current densities i.e. similar total enzymatic activity. Furthermore, the immobilized enzyme activity should be low enough to make the electrodes operate through the widest possible range of substrate concentrations with the turnover of the enzyme being rate limiting.

The voltammograms in the absence of substrate showed 20-25 mV peak to peak separation for either enzyme electrode. The slowest scan rate at which an Os^{3+} reduction wave became observable in the presence of substrate was 2 mVs^{-1} for GPO and 5 mVs^{-1} for LOX.

Figure 2 shows the current density as a function of substrate concentration in argon and in air. Because the electrodes were designed for equal current density and not for optimal electron transfer via the network to the electrode, oxygen competed effectively in the oxidation of the $FADH_2$ centers of LOX.

The pH dependence experiments were conducted in both STD buffer and universal buffer (.004 M each of sodium citrate, sodium barbitural, potassium phosphate and boric acid), with the pH being initially at 7.15 and then changed by the dropwise addition of 2 M HCl to about pH 4 and then to pH 10.5 with 2 M NaOH. The electrochemistry of the polymer in this pH range did not exhibit substantial differences. However at the extremes of the pH scale, we did observe changes in the peak separation and the height of the peaks, which were reversible upon pH restoration. Above pH 11, irreversible lowering of peak currents, increase in peak separation (50-100 mV) and diffusional tailing were observed. The changes in current between pH 4 and 10.5 were not totally reversible in GPO and LOX electrodes, but were reversible for GOX electrodes up to pH 10.5.

Figure 3 shows the pH dependence of the currents under anaerobic conditions at high substrate concentrations, where the current does not increase upon adding substrate. Incorporation of the enzyme in the redox epoxy network broadens the pH domains of maximum response and shifts these domains to higher pH. These effects are observed and are greatest in glucose oxidase, shown for comparison. In glucose electrodes the current remains within 20% of its maximum over the entire 6.5 - 10.5 pH range, with the maximum being at 7.5 - 9.0. In the case of LOX, the current is within 20% of its maximum over the 6.5 -8.5 pH range, the maximum being near pH 8; and in the case of GPO the flat region is at pH 7.5 - 8.5, peaking at about pH 8.2. The displacement of the pH maxima versus those of the free enzymes is of three pH units for GOX, 1.5 units for LOX, and .5 units for GPO. These differences in pH dependence will be discussed later.

Figure 4 shows the temperature dependence of the currents. The experiments were conducted at high substrate concentrations under argon. The Arrhenius current plots are reasonably

linear through the considered temperature range and the apparent activation energies are 59 KJ mol^{-1} for GPO and 79 KJ mol^{-1} for LOX electrodes.

Modified Eadie-Hofstee-type plots for the stationary electrode, at 50 rpm rotation and at >3500 rpm are shown in Figure 5. The often reported linear dependence is observed in the GPO electrode almost regardless of rotation speed. In the case of the LOX electrode the linearity is observed, however, only at high rotation speed (>4500 rpm).

The film thickness was determined by integrating the area of the quasi steady-state cyclic voltammogram for each electrode, and expressing the thickness as total amount of material /cm^2. The scan rate was 1 mV/s for electrodes up to 130 $\mu g/cm^2$ and .1 mV/s for thicker films. A second method for determining film thickness involved double step chronocoulometry , which was useful up to 130$\mu g/cm^2$. In the thinner films the results from such determinations were within 2% of the thicknesses calculated from the amount of polymer deposited on the film and the data from elemental analysis and UV spectrophotometry for the osmium content of the polymer. This indicates that almost all the polymer remains on the surface after immobilization. For thicker films the discrepancy increased to about 20% because of breakdown of the applicability of the methods, and not the loss of polymer after immobilization.

Figure 6 shows the variation of the intercepts of the modified Eadie-Hofstee plots as a function of the thickness of the enzyme containing redox epoxy network. The electrodes again are designed to have similar current densities at high substrate concentrations where a small change in concentration does not affect the current. The GPO and LOX electrodes' Eadie-Hofstee slopes are essentially independent of film thickness, being about 2.5 mM for GPO and 0.18 mM for LOX. The variation of the intercepts, i.e. current densities at infinite substrate concentrations with film thickness is linear at least through the 0-100 $\mu g\ cm^{-2}$ range for LOX containing redox epoxy networks and at least through the 0-200 $\mu g\ cm^{-2}$ for the GPO containing ones.

GPO electrodes have a much shorter shelf life than GOX electrodes. After 1 month storage at room temperature (~25°C) the electrodes retained only 10% of their activity, while GOX electrodes, after an initial loss associated with curing of the epoxy network, were stable. When catalase was coimmobilized on the electrode no substantial improvement was observed. Though dry GPO is quite stable, we observed severe deactivation upon storage in pH 8.1 HEPES buffer. Upon one month storage of the LOX electrodes at room temperature (~25°C) no current was retained.

The response times of the electrodes were studied by measuring the response of the electrodes to steps in concentration between 0 and 10 times the half saturation point . The studies were done in a 10 ml cell with the electrode rotating at different rotation rates under a N_2 atmosphere. In all cases the response times decreased with increasing electrode rotation rate, to our 4,000 rpm limit, where they dropped to 1-2 sec. Thus, we were measuring the mixing time

not the true response time of the electrodes. (As response time we define the time needed for the response to reach 90% of the saturation current.)

The results summarizing the performance of the "typical" electrode as a sensor are depicted in Table I.

Discussion. In enzyme electrodes with 3-dimensional redox polymer networks complexing, binding and electrically interconnecting the redox centers to electrodes, the following processes define the observed current :

$$E_{ox} + S \underset{k_{-1}}{\overset{k_1}{\rightleftharpoons}} ES \xrightarrow{k_2} E_r + P \qquad (1)$$

$$E_r + 2\,R_{ox} \xrightarrow{k_3} E_{ox} + 2\,R_r + 2\,H^+ \qquad (2)$$

$$R_{ox,w} + R_{r,w+1} \xrightarrow{D_{ct}} R_{r,w} + R_{ox,w+1} \qquad (3)$$

$$R_r \xrightarrow{\infty} R_{ox} \qquad (4)$$

Equation 1 represents in combination with equation 2 the reaction of the enzyme with the substrate (S) by a uni uni uni uni ping pong mechanism, accepted for GPO and GOX (*12,14*). The oxidized form of the enzyme (E_{ox}) forms the enzyme-substrate complex (ES) having an equilibrium constant k_{-1}/k_1. The complex dissociates with a rate constant k_2 into the reduced form of the enzyme (E_r) and product (P). At this stage, the enzyme can be reoxidized by oxygen according to :

$$E_r + O_2 \xrightarrow{k_o} E_{ox} + H_2O_2 \qquad (5)$$

Under anaerobic conditions, equation 2 describes the reoxidation process adequately. The reduced enzyme is subsequently oxidized by a sequence of two one-electron transfer steps. The electrons are transferred to the oxidized polymer bound relays (R_{ox}) , which are reduced with a rate constant k_3. Finally, electrons transfer through the redox polymer - enzyme network with an overall "electron diffusion coefficient" D_{ct} according to equation 3 which describes the succession of

electron transfer self-exchange reactions between neighboring redox sites (w, w+1). D_{ct} may increase exponentially with the cube root of concentration of redox centers, if the electron propagation is a percolative, phonon-assisted tunneling process, or quadratically (with the redox center's concentration) if the propagation involves chain segment collisions. The reoxidation of the relay at the electrode surface completing the second part of the catalytic cycle is fast.

An effort has been made to model and simulate this set of equations and solve for the catalytic current. Saveant (*18*) has solved the general case for a catalytic first order reaction on a polymer film. Gough (*19,20*) and others (*21-23*) have tried in the past to apply this analysis to enzyme electrodes. No analytical solution can be obtained for the general case even when a ping pong mechanism is not involved. However, in order to semiquantitatively interpret the results, we postulate that after applying Aris' (*24*) analysis to the problem at hand, one can write for the catalytic current :

$$j = \frac{\eta\, j_{max}}{1 + K_{rox}/C_{rt}} - \frac{K_S/a_S}{1 + K_{rox}/C_{rt}}\,\frac{j}{C_S} \qquad (6)$$

where j is the current density, η is an effectiveness factor, defined as the ratio of the actual current density over the current density that could be obtained under kinetic control, $j_{max} = 2\,FLk_2C_{Et}$, where F the Faraday constant, L the wet film thickness, C_{Et} the total enzyme concentration in the film, $K_{rox} = k_2/k_3$, $K_S = (k_2+k_{-1})/k_1$, a_S is the partition coefficient of the substrate in the film, C_{rt} is the relay concentration in the enzyme-polymer film, and C_S is the substrate concentration in the bulk solution.

Equation 6 looks deceptively simple. This is so because our inability to exactly describe the process has been hidden in the effectiveness factor. Were we able to describe rigorously the coupled processes, η would be the solution of the differential equations describing the reactions of equations 1-4. In this case η would depend on all the parameters in equation 6, on D_{ct} and on the diffusion coefficient of the substrate. η cannot assume a closed form solution unless simplifying assumptions, negating the very purpose of mathematically describing the process, are made. When equation 6 is plotted in the usual Eadie-Hofstee form of j vs j/C_S, the plot is rarely a straight line. Unless there is an unusual coincidence of parameter values a linear plot is not obtained, i.e. $\eta \neq 1$ unless the current is not limited by either substrate or electron diffusion. Such plots can be used as a semiquantitative diagnostic test for the characterization of immobilized enzymes in general (*25,26*) Experimentally one can distinguish between substrate diffusion limitations and electron diffusion limitations by varying the electrode rotation rate. Above some

rotation rate, no external diffusion limitation will prevail. In the absence of internal substrate diffusion limitation and of electron diffusion limitation, the plots become linear at sufficiently high rotation rates. At this point, the current observed is the kinetic current (described by equation 6 when $\eta=1$). There are additional postulates in equation 6 which will be discussed.

Effectiveness of Electrical Communication via the 3-Dimensional Network. In designing the 3-dimensional enzyme containing redox polymer network, we seek to transfer electrons from the enzyme redox centers to the network and through the network to the electrode, at rates exceeding the maximum rate of electron transfer from the substrate to the redox centers of the enzyme, i.e. the turnover number of the enzyme. When the transfer of electrons from the substrate to the network is fast enough to maintain a sufficiently high steady state Os^{2+}/Os^{3+} ratio, i.e. to make the Nernst potential of the film reducing relative to the formal potential, only an oxidation current is observed in slow scan rate cyclic voltammograms. This oxidation current will be maintained until the ratio Os^{2+}/Os^{3+} decreases, because the rate of supply of electrons to the network from the substrate through the enzyme cannot match the rate of oxidation of the network on the electrode. At this point, the Nernst potential of the network will become sufficiently positive for a reduction current to appear at a reducing potential relative to the formal potential of the network. This situation will arise at or above a scan rate related to the turnover rate of the enzyme and its relationship to the efficiency with which electrons are transferred from the enzyme to and through the network. As seen in Fig. 1c for GPO this rate is $2mVs^{-1}$ and for LOX it is $5mVs^{-1}$. For glucose electrodes designed to exceed in their enzyme activity (and current density) the LOX and GPO electrodes, critical scan rates are of $20mVs^{-1}$. For the same enzyme concentration in the film, the increasing critical scan rates reflect the increasing turnover numbers for these enzymes and/or the increasing effectiveness of communication via the network.

Under anaerobic conditions both the critical scan rate and the current density reflect qualitatively the relative rates of enzymatic turnover (process described by equation 1) and the effectiveness of communication (process described by equations 2 and 3). Under aerobic conditions, the current density and the suppression of current relative to anaerobic conditions qualitatively reflect the effectiveness of communication relative to the rate of electron transfer from the enzyme to O_2 (process described by equation 5). As seen in Fig. 2, O_2 competes more effectively for reduced LOX electrons than for reduced GPO electrons. This fact may signify a higher k_3 for GPO than for LOX, and/or a higher k_O for LOX than for GPO (refer to equations 2 and 5).

pH Dependence. The pH dependence of the current in "wired" GOX, LOX, or GPO differs from the pH dependence of the enzyme-catalyzed oxidation of the substrates by O_2; the maxima are shifted to higher pH and the peaks are broader. These effects might be explained as follows :

At higher pH the polyanionic enzyme-polycationic polymer complexes are tighter because the enzyme has a greater net negative charge when its bases are deprotonated and its acids ionized. Because of the tighter binding in the complex, the electron transfer distances are shorter and the electron transfer rates faster. The broadening in the pH maxima of the current densities (Figure 3) reflects the balancing of the enhanced electron transfer and the reduced enzyme activity with increasing pH.

A similar argument based on electrostatics accounts for the different pH dependences when equation 2 represents the rate limiting step of the process. The Os^{3+} relays abstract electrons from either fully reduced ($FADH_2$) or from the (FADH·) radical, transiently present because of single electron transfer to Os^{3+}. The pK_a of both of these species is between 6 and 7 in unbound FAD (27) and is also between 6 and 7 for GPO and GOX (15,28) and in FMN dependent LOX (29). Thus, above pH 7 the species from which Os^{3+} accepts electrons have a negative charge. The increased electrostatic attraction between the donor and the acceptor at higher pH again shortens the electron transfer distance and increases the rate of electron transfer. In contrast, higher pH causes a decrease in the rate of the formation of the peroxo adduct (28,30,31) formed upon oxidation of the enzyme by O_2.

Diffusional Effects. As discussed earlier, linearity of Eadie-Hofstee plots is unlikely when $\eta \neq 1$ (Equation 6). The condition $\eta = 1$ requires, among other requirements, also that substrate transport to the film not limit the electrode kinetics. When substrate diffusion to the electrode does limit the electrode kinetics, i.e. at sufficiently slow rotation rates the plots are non-linear (Figure 5). When the enzyme loading is high and/or when its turnover rate is rapid, mass transport can limit the electrode kinetics even at high rotation rates and the Eadie-Hofstee plots remain non-linear even for the fastest rotating electrodes (4500 rpm).

When linear, the intercept of the Eadie-Hofstee plots is expected to be proportional to the amount of active enzyme in electrical contact with the electrode. As long as the electrical communication is maintained, the Eadie-Hofstee intercept is expected to be proportional to film thickness. The Eadie-Hofstee slopes should, however, be independent of film thickness when the concentration of polymer and enzyme in the film remain constant. As seen in Figure 6, the slopes are indeed independent of film thickness and the intercepts are proportional to film thickness in both GPO and LOX electrodes. At zero film thickness the intercepts should, however, be nil. That this is not exactly the case reveals a small systematic error in our estimate of film thickness.

The slope of the Eadie-Hofstee plots represents the apparent K_m of the electrodes and is near 3mM for the GPO and 0.2mM for the LOX electrodes analyzed. The slopes, i.e. the apparent K_m values, can be readily varied over a wide range by changing the enzyme/polymer ratio. Though we do not show this in the results, the slopes have been increased by an order of magnitude in both electrodes by increasing the enzyme/polymer ratio. As expected, when the ratio

was increased, the Eadie-Hofstee plots became non-linear even at high electrode rotation rates. Evidently, either diffusional substrate transport or electron diffusion in the electrically insulating enzyme-enriched network and not the enzyme's turnover capacity now controlled the electrode kinetics.

Acknowledgments. We thank Mr Henry Franklin, director of the Mechanical Engineering Department workshop for fine craftsmanship in building our apparatus; Dr Takis Argitis for SEM data; Dr Danli Wang for sharing preliminary results on the stabilization of LOX; Lois Davidson for the purification of LOX; One of us (IK) thanks Dr Brian A. Gregg, now at NREL, for guidance; Dr Alan Hauser, now at the University of Hawaii, for sharing his painstaking derivation of a model describing the electrode response; and Dr Adrian Michael, now at the University of Pittsburgh for a stimulating debate on the process of electron transfer in redox polymer films.

LITERATURE CITED

1. Hale, P.D.; Inagaki, T.; Karan, H.I.; Okamoto, Y.; Skotheim, T.A. *J. Am. Chem. Soc.* **1989**, 111, 3482-3.
2. Hale, P.D.; Boguslavski, L.I.; Inagaki, T.; Lee, H.S.; Skotheim, T.A.; Karan, H.I.; Okamoto, Y. *Mol. Cryst. Liq. Cryst.* **1990**, 190, 251-8.
3. Hale, P.D.; Boguslavski, L.I.; Inagaki, T.; Karan, H.I.; Lee, H.S.; Skotheim, T.A.; Okamoto, Y. *Anal. Chem.* **1991**, 63, 677-82.
4. Foulds, N.C.; Lowe, C.R. *Anal. Chem.*, **1988**, 60, 2473-8.
5. Cenas, N.K.; Pocius, A.K.; Kulys, J.J. *Bioelectrochem. Bioenerget.* **1984**, 12, 583-91.
6. Degani, Y.; Heller, A. *J. Am. Chem. Soc.* **1989**, 111, 2357-8.
7. Gregg, B.A.; Heller, A. *Anal. Chem.* **1990**, 62, 258-63.
8. Pishko, M.V.; Katakis, I.; Lindquist, S-L.; Ye, L.; Gregg, B.A.; Heller, A. *Angew. Chem., Int. Ed. Engl.* **1990**, 29, 82-4.
9. Pishko, M.V.; Katakis, I.; Lindquist, S-L.; Degani, Y.; Heller, A. *Mol. Cryst. Liq. Cryst.* **1990**, 190, 221-49.
10. Gregg, B.A.; Heller, A. *J. Phys. Chem.* **1991**, 95, 5970 - 5.
11. Gregg, B.A.; Heller, A. *J. Phys. Chem.* **1991**, 95, 5976 - 80.
12. Nakamura, S.; Fujuki, S.J. J. Biochem. **1968**, 63, 51-7.
13. Gibson, Q.H.; Swoboda, B.E.P.; Massey, V. *J. Biol. Chem.* **1964**, 239, 3927-34.
14. Jacobs, N.J.; VanDemark, P.J. *Arch. Biochem. Biophys.* **1960**, 88, 250-5.

15. Claiborne, A. *J. Biol. Chem.* **1986**, 261(31), 14398-407.

16. Bio-Rad Protein Assay. Manufacturer's manual, Bio-Rad, Richmond, CA, 1991.

17. Finnsugar Biochemicals Inc. *Enzymes for Diagnostic Reagents Technical Information Catalog*; Sigma Chemical Co. Product No. G-7141 technical information publication, Sigma Chemical Co, St. Louis, MO, 1991.

18. Andrieux, C.P.; Dumas-Bouchiat, J.M.; Saveant, J.M. *J. Electroanal. Chem.* **1982**, 131, 1-35.

19. Leypoldt, J.K.; Gough, D.A. *Anal. Chem.* **1984**, 56, 2896-904.

20. Tse, P.H.S.;Leypoldt, J.K.; Gough, D.A. *Biotechnol. Bioeng.* **1987**, 29, 696-704.

21. Mell, L.D.; Malloy, J.T. *Anal. Chem.* **1975**, 47(2), 299-307.

22. Ikeda, T.; Miki, K.; Senda, M. *Anal. Sci.* **1988**, 4, 133 - 8.

23. Yokoyama, K.; Tamiya, E.; Karube, I. *J. Electroanal. Chem.* **1989**, 273, 107 - 17.

24. Aris, R. *Mathematical Theory of Diffusion and Reaction in Permeable Catalysts*; Oxford University Press: London, 1975, pp 348-80.

25. Engasser, J.M.; Horwath, C. In *Immobilized Enzyme Principles*; Wingard, L.B.Jr.; Katchalski-Katzir, E.; Goldstein, L., Eds; Applied Biochemistry and Bioengineering; Academic Press Inc.: N. York, N.Y., 1976, Vol. 1; pp 127 - 200.

26. Goldstein, L. *Meth. Enzymol.* **1976**, 44, 397 - 450.

27. Dryhurst, G. *Electrochemistry of Biological Molecules*; Academic Press : N. York, 1977, p 371.

28. Stankovich, M.T.; Schopfer, L.M.; Massey, V. *J. Biol. Chem.* **1978**, 253(14), 4971-9.

29. Stankovich, M.; Fox, B. *Biochemistry* **1983**, 22, 4466-72.

30. Ghisla, S.; Massey, V. *Eur. J. Biochem.* **1989**, 181, 1-17.

31. Hemmerich, P.; Knappe, W-R.; Kramer, H.E.A.; Traber, R. *Eur. J. Biochem.* **1980**, 104, 511-20.

Brief

Redox centers of glycerol-3-phosphate oxidase (GPO) and lactate oxidase (LOX) were electrically connected by hydrophylic redox epoxy networks to electrodes. Diffusional processes can be suppressed with appropriate manipulation of the eelctrode construction parameters. Both electrodes are fast (0-90% risetime <2sec) and sensitive (GPO - 0.02A $M^{-1}cm^2$, LOX - 0.3A $M^{-1}cm^{-2}$).

CREDIT

We acknowledge support of this work by the Office of Naval Research, The National Science Foundation, and the Welch Foundation.

Table I. GPO & LOX Electrode Characteristics

	GPO	LOX
Half saturation point (mM)	2.6 +/- .3	.16 +/- .02
Current density at "K_m" ($\mu A/cm^2$)	45 +/- .5	60 +/- .3
Sensitivity in ($A\ M^{-1}cm^{-2}$)	.02 +/- .002	.3 +/- .01
Half saturation current/background current/ratio	32	43
% current loss at half saturation in air[1]	8 +/- 1	39 +/- 5

[1]Comparison between Argon and air saturated solutions (0 and .2 mM [O_2] respectively).

Figure Captions

Figure 1. Cyclic voltammograms demonstrating the catalytic nature of the anodic currents and the "threshold" or breakpoint in scan rate for the appearance of reductive waves. Scans (a) 1 mV/s, in STD buffer, (b) 1 mV/s after the introduction of 10 times the half saturation point substrate concentration, (c) lowest scan rate value where reduction wave appears : GPO 2 mV/s, LOX 5 mV/s. Electrode construction parameters : Typical, thickness : 130 $\mu g/cm^2$. All electrodes had diameter 3 mm and were rotated at highest rotation rate for linear E-H plots.

Figure 2. Dependence of the current on substrate concentration. The insert shows the fraction of the current remaining after the argon-purged solution is air saturated, as a function of the substrate concentration expressed in multiples of the apparent Km of the electrodes. 130 μgcm^{-2} film thickness; STD buffer, electrodes rotated at 3000 rpm.

Figure 3. pH dependence of the activity of the native enzymes in solution and of the response of the electrodes. The electrodes were rotated at 1000 rpm in Argon saturated solutions at saturating substrate concentrations.

Figure 4. Temperature dependence of the current. Rotation rate was 2000 rpm; film thickness 20 μgcm^{-2}; STD buffer; saturating substrate concentrations.

Figure 5. Eadie-Hofstee plots at varying angular velocities. STD buffer, 21.7 ^oC, argon saturated solution, film thickness 130 μgcm^{-2}.

Figure 6. (a). Variation of the intercepts of the modified Eadie - Hofstee plots with thickness. The intercepts were calculated from plots similar to those in Figure 5 for each electrode. (b). Variation of the slope of the Eadie - Hofstee plots (calculated similarly), with thickness.

Fig. 1 ACSM24

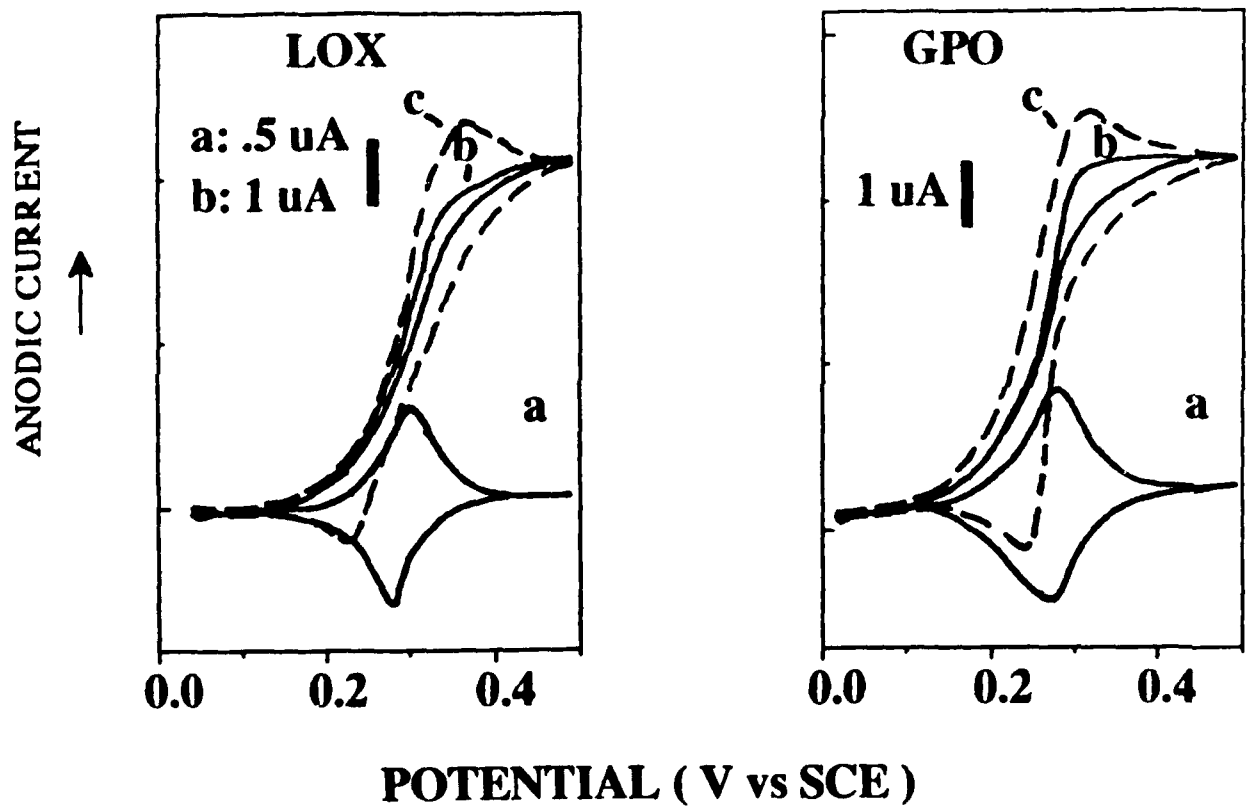
LOX
a: .5 uA
b: 1 uA
c
b
a
GPO
1 uA
c
b
a
ANODIC CURRENT
0.0
0.2
0.4
0.0
0.2
0.4
POTENTIAL (V vs SCE)

Fig. 2 ACSM24

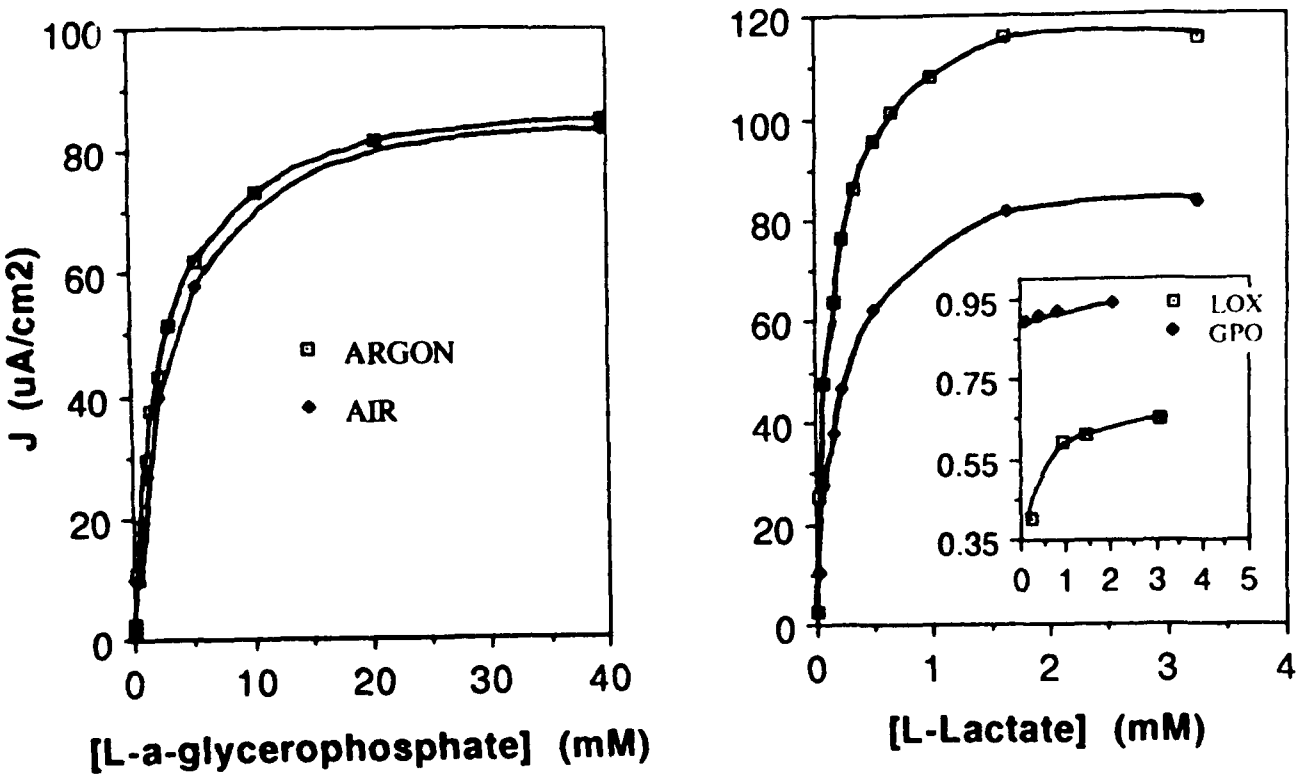

Fig 2 ACSM24

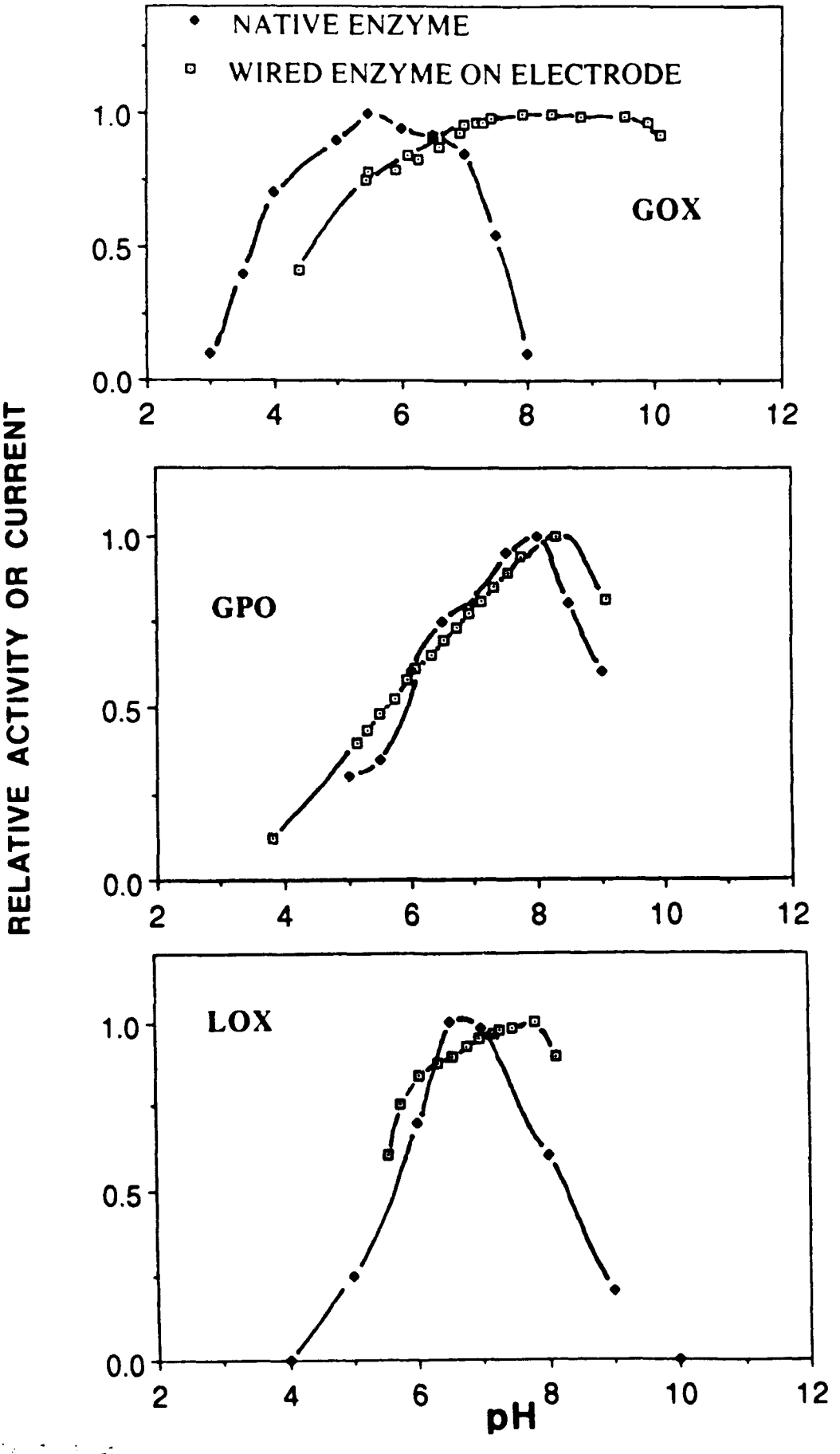
NATIVE ENZYME
WIRED ENZYME ON ELECTRODE
GOX
GPO
LOX
RELATIVE ACTIVITY OR CURRENT
pH
0.0
0.5
1.0
2
4
6
8
10
12

Fig. 3 ACSM24

Fig. 4 ACSM24

60%

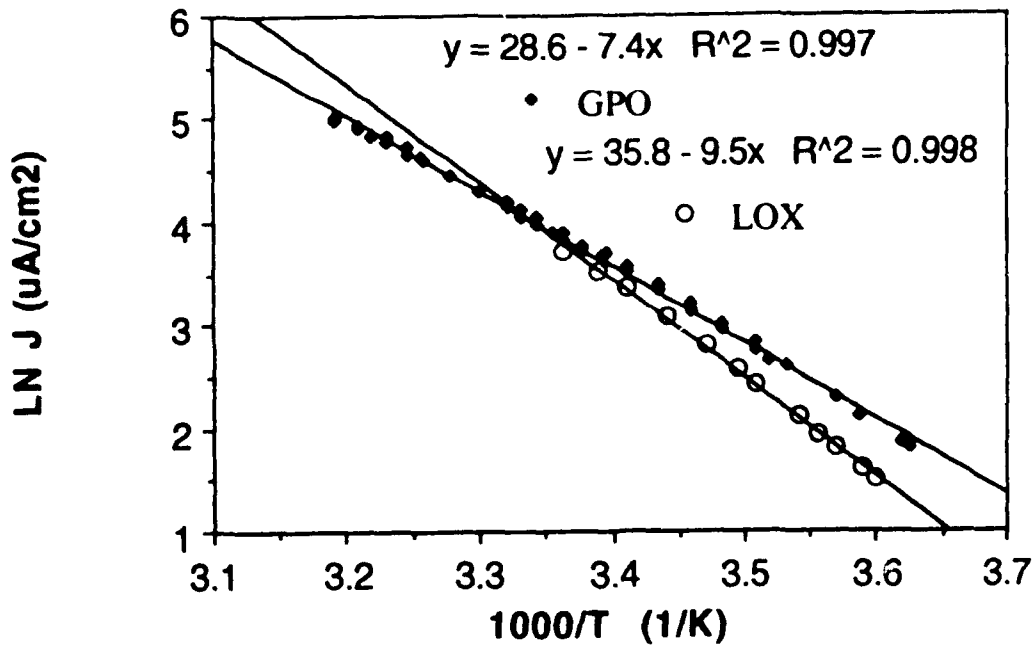

Fig. 4

ACSM 24

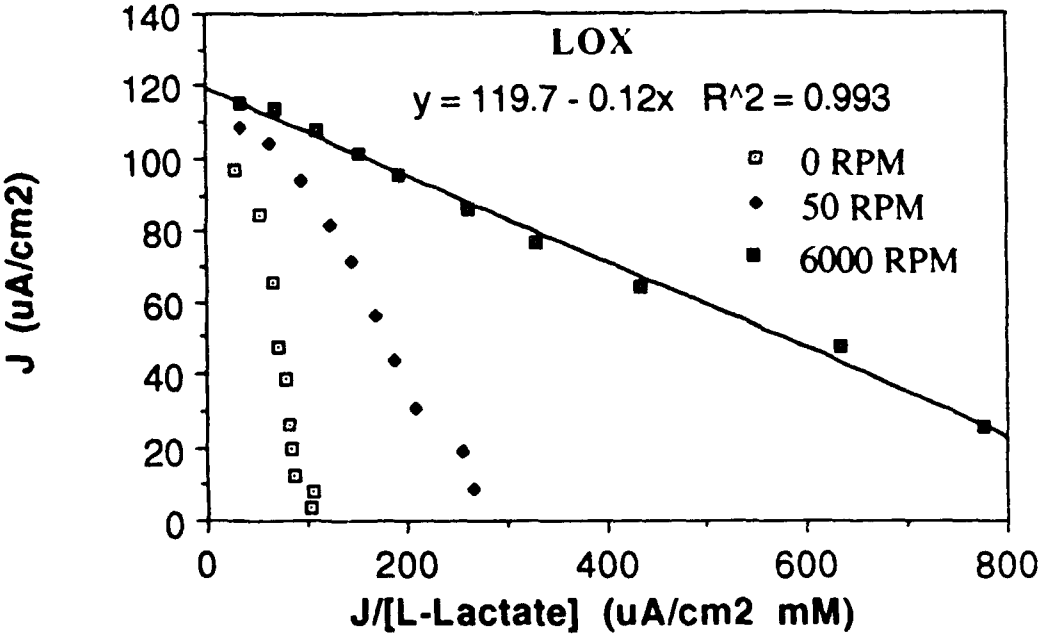

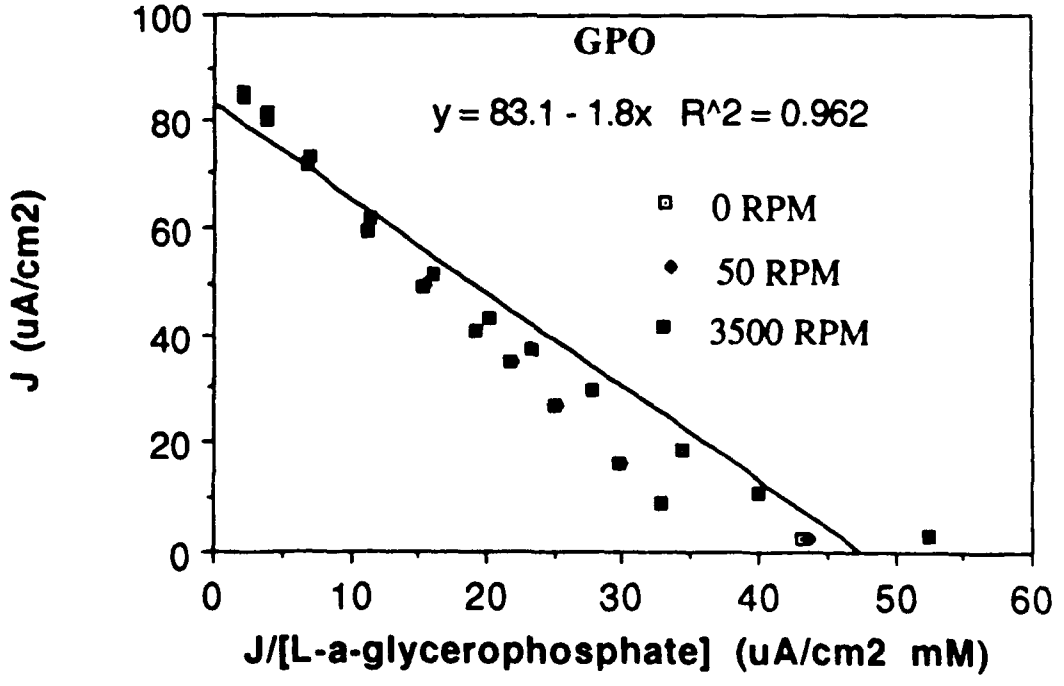

Fig. 5 AC5M24

Fig. 6 AC5M24

a

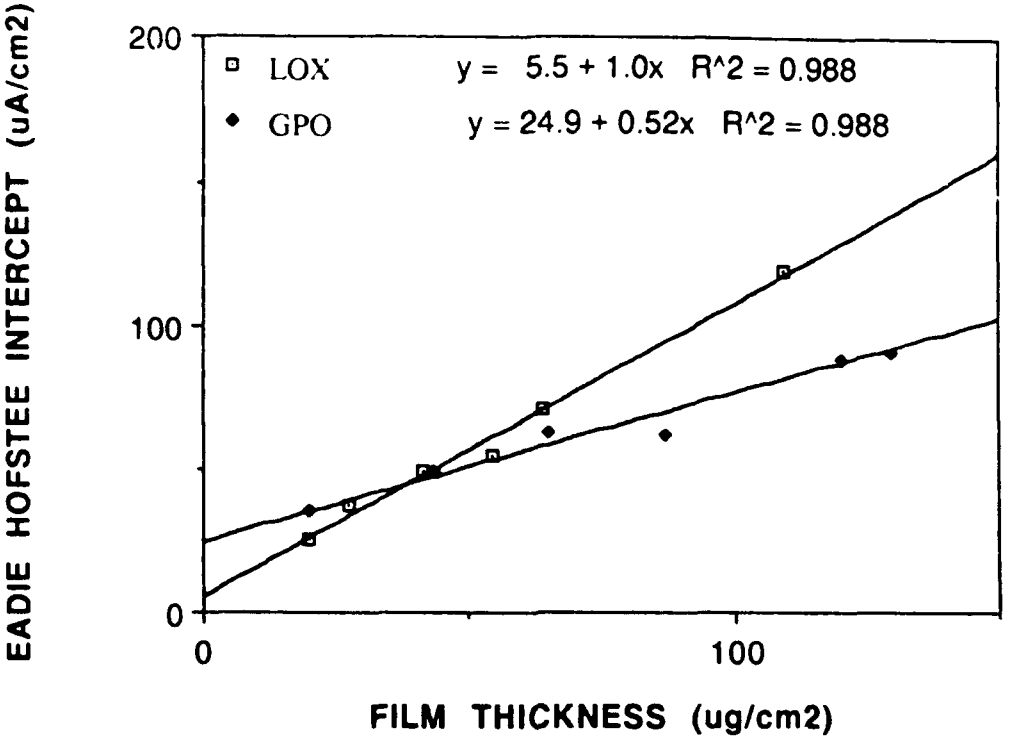

b

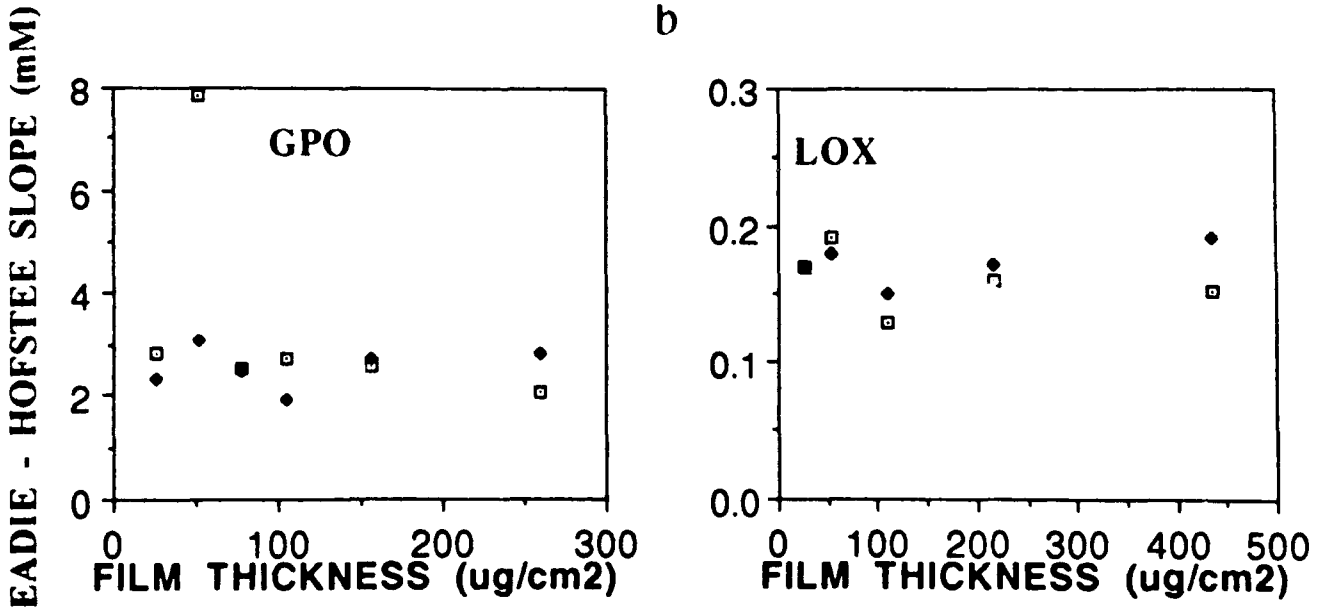

Fig. 6 ACSM24